Australian Journal of Basic and Applied Sciences, 5(8): 766-770, 2011
ISSN 1991-8178

An Impact of the Hole Etching Depth Within a Photonic Crystal VCSEL on its Heat Sources

[1]Saeid Marjani, [2]Rahim Faez and [1]Hamid Marjani

[1]Department of Electrical Engineering, Arak Branch, Islamic Azad University, Arak, Iran.
[2]Department of Electrical Engineering, Sharif University of Technology, Tehran, Iran.

Abstract: In the present paper, for the first time, an impact of the hole etching depth within a photonic crystal vertical cavity surface emitting diode laser (PhC VCSEL) on its heat sources is analyzed discussed. The device employs InGaAsP multi-quantum wells sandwiched between GaAs/AlGaAs and GaAs/AlAs distributed Bragg reflectors (DBRs) modeled using a numerical simulator. The basic design goal was the study of the various elements of heat sources upon the hole etching depth, including the total heat power, the Joule heat power, the Peltier-Thomson heat power and the Recombination heat power.

Key words: Modeling, Hole etching depth, Heat sources, PhC VCSEL

INTRODUCTION

In recent years, the vertical cavity surface emitting lasers have attracted extremely (Iga, 2000). VCSEL is one of the key light source used in high performance optical communication systems where single mode operation, high output power, high speed modulation and low manufacture cost are necessary (Dems *et al.,* 2005). High optical gain in the active area and high thermal conductivity in the reflecting mirrors are the main difficulties in developing VCSELs which are used in the field of optical spectroscopy (Kapon and Sirbu, 2009).

Lattice heat is generated whenever physical processes transfer energy to the crystal lattice. According to differences in transfer mechanisms, heat sources can be separated into Joule heat, electron–hole recombination heat, Thomson heat, and heat from optical absorption. Self-heating often limits the performance of optoelectronic devices. Heat is generated when carriers transfer part of their energy to the crystal lattice. In consequence, the thermal energy of the lattice rises, which is measured as an increase in its temperature (Piprek, 2003). The simultaneous demonstration of high temperature, high power lasing is the main challenge in developing VCSELs (Piprek *et al.,* 2004). In this paper, we employ numerical-based simulation software to assist in the device design and simulation (SILVACO, 2010).

In this paper, we introduced the effects of the hole etching depth on various elements of heat sources within the active region of a photonic crystal VCSEL.

In the following, we first briefly describe the numerical model. Next the details of the PhC VCSEL structure are introduced, and we present the obtained numerical results. Finally, the conclusions provide common guidelines for designing performance of PhC VCSELS.

Theory:

In simulation VCSEL, we must consider the electrical, optical and thermal interaction during VCSEL performance. Base of simulation is to solve Poisson and continuity equations for electrons and holes (SILVACO, 2010). Poisson's equation is defined by:

$$\nabla \bullet \left(\in \nabla \Psi \right) = \rho \tag{1}$$

where ψ is electrostatic potential, ρ is local charge density and ε is local permittivity. The continuity equations of electron and hole are given by (Piprek, 2003):

$$\frac{\partial n}{\partial t} = G_n - R_n + \frac{1}{q} \nabla . \vec{J}_n \tag{2}$$

Corresponding Author: Saeid Marjani, Department of Electrical Engineering, Arak Branch, Islamic Azad University, Arak, Iran.
E-mail: saeidmarjani@yahoo.com

$$\frac{\partial p}{\partial t} = G_p - R_p + \frac{1}{q}\nabla.\vec{J}_p \tag{3}$$

where n and p are the electron and hole concentration, J_n and J_p are the electron and hole current densities, G_n and G_p are the generation rates for electrons and holes, R_n and R_p are the recombination rates and q is the magnitude of electron charge.

The fundamental semiconductor equations (1)-(3) are solved self-consistently together with Helmholtz and the photon rate equations. The applied technique for the solution of Helmholtz equation is based on the improved effective index model (Hadley, 1995), which shows accuracy for the great portion of preliminary problems. This model is very well adapted to simulation of VCSEL structures, and it is often called effective frequency method (Wenzel and Wunsche, 1997). Two-dimensional Helmholtz equation is solved to determine the transverse optical field profile, and it is given by (SILVACO, 2010):

$$\nabla^2 E(r,z,\varphi) + \frac{\omega_0}{c^2}\varepsilon(r,z,\varphi,\omega)E(r,z,\varphi) = 0 \tag{4}$$

where ω is the frequency, ε(r, z, φ, ω) is the complex dielectric permittivity, E(r, z, φ) is the optical electric field and c is the speed of light in the vacuum.

The light power equation relates electrical and optical models. The photon rate equation is given by (SILVACO, 2010):

$$\frac{dS_m}{dt} = (\frac{c}{N_{eff}}G_m - \frac{1}{\tau_{ph_m}} - \frac{cL}{N_{eff}})S_m + R_{sp_m} \tag{5}$$

where S_m is the photon number, G_m is the modal gain, R_{sp_m} is the modal spontaneous emission rate, L represents the losses in the laser, N_{eff} is the group effective refractive index, τ_{ph_m} is the modal photon lifetime and c is the speed of light in the vacuum. The m refers to modal number. The modal gain is (SILVACO, 2010):

$$G_m = \iiint g_m(r,z).\left|E_m(r,z)\right|^2 rd\theta drdz \tag{6}$$

where $E_m(r, z)$ is the normalized optical field.

And modal of spontaneous emission rate is (SILVACO, 2010):

$$R_{sp_m} = \iiint r_{sp}(r,z)_m rd\theta drdz \tag{7}$$

The modal photon lifetime, τ_{ph_m}, determines losses in laser and it is given by (SILVACO, 2010):

$$\frac{1}{\tau_{ph_m}} = \frac{c}{NEFF}\left(\alpha_{a_m} + \alpha_{fc_m} + \alpha_{mir}\right) = \frac{c}{NEFF}G_m - \omega_0.\nu_{lm} \tag{8}$$

where α_a is losses of bulk absorption, α_{fc} is losses of free-carriers, α_{mir} is losses of mirrors and υ_{lm} is a parameter of dimensionless frequency.

The heat flow equation has the form (SILVACO, 2010):

$$C\frac{\partial T_L}{\partial t} = \nabla(\kappa\nabla T_L) + H \tag{9}$$

where C is the heat capacitance per unit volume, κ is the thermal conductivity, H is the generation, T_L is the local lattice temperature and H is the heat generation term.

The heat generation equation has the form (SILVACO, 2010):

$$H = [\frac{\overrightarrow{\left|J_n\right|}^2}{q\mu_n n} + \frac{\overrightarrow{\left|J_p\right|}^2}{q\mu_p p}] + q(R-G)[\phi_p - \phi_n + T_L(P_p - P_n)] - T_L(\overrightarrow{J_n}\nabla P_n + \overrightarrow{J_p}\nabla P_p) \tag{10}$$

where:

$[\frac{\overrightarrow{|J_n|}^2}{q\mu_n n} + \frac{\overrightarrow{|J_p|}^2}{q\mu_p p}]$ is the Joule heating term,

$q(R-G)[\phi_p - \phi_n + T_L(P_p - P_n)]$ is the recombination and generation heating and cooling term,

$-T_L(\overrightarrow{J_n}\nabla P_n + \overrightarrow{J_p}\nabla P_p)$ accounts for the Peltier and Joule-Thomson effects.

Equations (1)-(10) provide an approach that can account for the mutual dependence of electrical, thermal, optical and elements of heat sources. In this paper, we employ numerical-based simulation software to assist in the device design and optimization (SILVACO, 2010).

VCSEL Structure:

Fig.1 shows the schematic structure of PhC VCSEL device, which is modified from the experimental device developed in the past (Babic *et al.,* 1997). The VCSEL device consists of an active region consists of six quantum wells where the well is 5.5nm $In_{0.76}Ga_{0.24}As_{0.82}P_{0.18}$ and the barrier is 8nm $In_{0.48}Ga_{0.52}As_{0.82}P_{0.18}$. In both sides of this active region, there is InP and on top of it GaAs. 30 layers of the top mirror are made of GaAs/$Al_{0.33}Ga_{0.67}As$ with index of refraction of layers 3.38 and 3.05 respectively and 28 layers of the bottom mirror are made of GaAs/AlAs with index of refraction of layers 3.38 and 2.89 respectively.. Triangular-lattice air holes are formed in the upper pairs of top DBR. The optical confinement is achieved by means of seven air holes where the center is missed off to make the defect region, as shown in Fig.2. The PhC design parameter is connected by hole etch depth, dE.

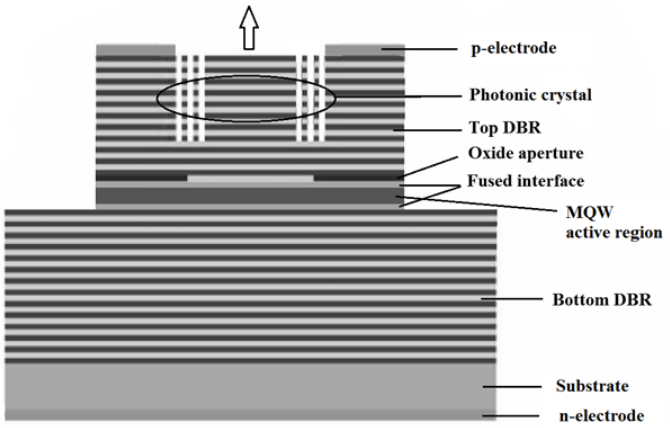

Fig. 1: Schematic structure of the VCSEL device.

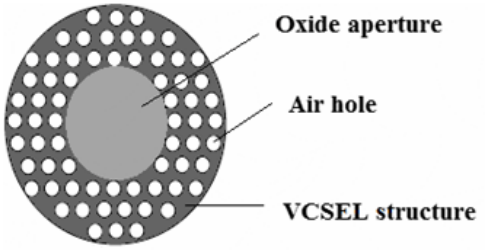

Fig. 2: Top view of the triangular-lattice air holes pattern.

Results:

In the present work, the effect of the hole etching depth on various elements of heat sources is analyzed and discussed. Fundamentally, the heat power peaks at the MQW region for all heat source elements. The highest contributor of heat power comes from the Peltier-Thomson heat power followed by the recombination heat power and finally the joule heat power.

Fig.3 shows the total heat power within a vertical cross-section of the active region at an output power of 9mW. As can be seen from Fig.3, increasing of the hole etching depth causes the reduction of the total heat power which should be mainly due to lower current density in Pout=9mW.

Table 1 shows the maximum of various elements of heat sources upon the hole etching depth, including the total heat power, the Joule heat power, the Peltier-Thomson heat power and the Recombination heat power at output power of 9mW. As can be seen from Table 1, increasing of the hole etching depth causes the reduction of the joule heat power which should be mainly due to lower current density in Pout=9mW. As shown in the Table 1, when the hole etching depth increases, the Peltier-Thomson heat power shows the same rule as that at the joule heat power which should be mainly due to lower current density. Peltier-Thomson heat is transferred between carriers and lattice as current flows along a gradient of the thermoelectrical power, and it changes with the density of states, carrier concentration, and temperature. When electrons enter a material with under conduction band edge, they suddenly display extra kinetic energy (hot electrons) that is finally scattered to the lattice. Vice versa, electrons need to receive additional energy from the lattice to leave the quantum well. For that reason, Thomson heat can be positive or negative. It can be found that the increment of the hole etching depth from 2 to 6 μm, leads to the upper recombination heat power at an output power of 9mW, which should be mainly due to upper net recombination rate, including thermal generation of carriers.

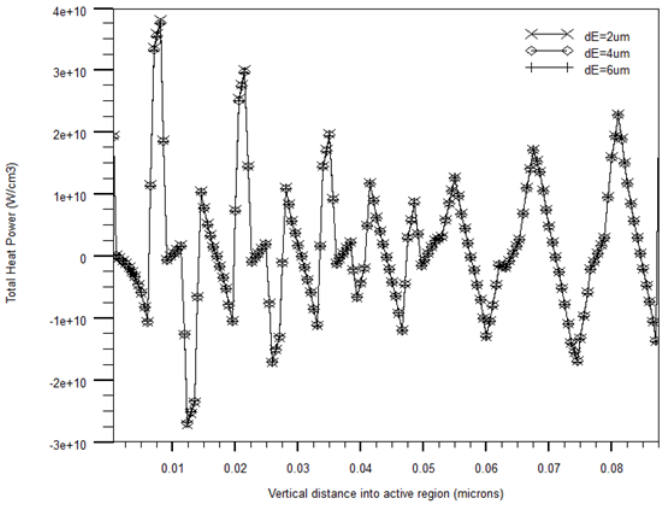

Fig. 3: effect of Hole Etching Depth on the total heat power within the active region.

Table 1: The maximum of various elements of heat sources upon the hole etching depth, including the total heat power, the Joule heat power, the Peltier-Thomson heat power and the Recombination heat power at output power of 9mW.

various elements of heat sources	dE=2um	dE=4um	dE=6um
Maximum total heat power	3.8130e10 W/cm3	3.7751e10 W/cm3	3.7581e10 W/cm3
Maximum joule heat power	6.5069e7 W/cm3	6.3156e7 W/cm3	6.3127e7 W/cm3
Maximum Peltier-thomson heat power	3.7610e10 W/cm3	3.7229e10 W/cm3	3.7060e10 W/cm3
Maximum recombination heat power	5.0870e8 W/cm3	5.1080e8 W/cm3	5.1139e8 W/cm3

Conclusion:

In this paper, we present the effects of the hole etching depth on various elements of heat sources within the active region of a long wavelength InGaAsP photonic crystal VCSEL. In summary, increasing of the hole etching depth, decreases the joule and Peltier-Thomson heat powers but increases the recombination heat power into MQW region at output power of 9mW. The maximum total heat power of the hole etching depth 2um, 4um, and 6um are 3.813e10 W/cm3, 3.7751e10 W/cm3, and 3.7581e10 W/cm3, respectively at output power of 9mW. The results indicate that the highest contributor of heat power comes from the Peltier-Thomson heat power (up to 3.761e10 W/cm3) followed by the recombination heat power (up to 5.1139e8 W/cm3) and finally the joule heat power (up to 6.5069e7 W/cm3).

REFERENCES

Babic, D.I. and J.S. Piprek, K. Mirin, R.P. Margalit, N.M. Mars, D.E. Bowers, J.E. Hu, E.L. "Design and analysis, 1997. of double-fused 1.55-μm vertical-cavity lasers, " IEEE J. Quantum Electron., 33: 1369-1383.

Dems, M., R. Kotynski and K. Panajotov, 2005. "Plane Wave Admittance Method - a novel approach for determining the electromagnetic modes in photonic structures," J. Opt. Express, 13: 3196-3207.

Hadley, G.R., 1995. "Effective index model for vertical-cavity surface-emitting lasers," J. of Opt. Lett., 20(13): 1483-1485.

Iga, K., 2000."Surface-emitting laser—its birth and generation of new optoelectronic field," IEEE J. Sel. Topics Electron, 6: 1201-1215.

Kapon, E., A. Sirbu, 2009. "Power-efficient answer," Nature Photonics., 3: 27-29.

Piprek, J., 2003. "Semiconductor Optoelectronic Devices: Introduction to Physics and Simulation, " Chap. 3 Carrier Transport and Chap. 6 Heat Generation and Dissipation UCSB: Academic Press, pp: 49-50: 141-147.

Piprek, J., M. Mehta and V. Jayaraman, 2004. "Design and Optimization of high-performance 1.3 um VCSELs, " Proc. of SPIE5349.

SILVACO International Incorporated, 2010. "ATLAS User's Manual", Version 5.12.0.R. USA, SILVACO, Inc.

Wenzel, H., H.-J. Wunsche, 1997. "The effective frequency method in the analysis of vertical-cavity surface-emitting lasers," IEEE J. Quantum Electronics., 33: 1156.